arXiv:1508.04517v1 [cond-mat.soft] 19 Aug 2015

Dynamics and instantaneous normal modes in a liquid with density anomalies

M P Ciamarra[1,2] **and P Sollich**[3]

[1] Division of Physics and Applied Physics, School of Physical and Mathematical Sciences, Nanyang Technological University, Singapore

[2] CNR–SPIN, Dipartimento di Scienze Fisiche, Università di Napoli Federico II, I-80126, Napoli, Italy

[3] King's College London, Department of Mathematics, Strand, London WC2R 2LS, United Kingdom

Abstract. We investigate the relation between the dynamical features of a supercooled liquid and those of its potential energy landscape, focusing on a model liquid with density anomalies. We consider, at fixed temperature, pairs of state points with different density but the same diffusion constant, and find that surprisingly they have identical dynamical features at all length and time scales. This is shown by the collapse of their mean square displacements and of their self–intermediate scattering functions at different wavevectors. We then investigate how the features of the energy landscape change with density, and establish that state points with equal diffusion constant have different landscapes. In particular, we find a correlation between the fraction of instantaneous normal modes connecting different energy minima and the diffusion constant, but unlike in other systems these two quantities are not in one–to–one correspondence with each other, showing that additional landscape features must be relevant in determining the diffusion constant.

PACS numbers: 61.43.Fs,66.10.Cb,61.20.Lc

Submitted to: *jpcm*

1. Introduction

Particle motion in glassy systems is frequently conceptualized as consisting of caging periods, during which the system rattles around in a energy minimum of its energy landscape, interrupted by transitions between minima. In this scenario the features of the potential energy landscape (PEL) play a fundamental role in determining the overall dynamical properties. One way to investigate how a system explores its PEL is via the study of the instantaneous normal modes (INM) [1], which are the instantaneous eigenvalues and eigenvectors of the Hessian matrix. The eigenvalues give information about the curvatures of the PEL hypersurface around the point the system is visiting, while the eigenvectors give the corresponding directions for the joint motion of particles through phase space. As concerns the dynamical features of the system, the negative eigenvalues are of particular interest as they identify the unstable modes of the system [2, 3]. Specifically, some of these negative eigenvalues are expected to be directly related to diffusion. It is clear, however, that not all of the unstable modes can contribute to diffusion as unstable modes are also observed at temperatures which are sufficiently low for the diffusion constant to be negligible. Strategies must therefore be devised to determine which are the unstable modes that are relevant to particle diffusion [4, 5, 6].

Here we explore a proposal by La Nave and coworkers [5], who suggested that the unstable modes allowing for diffusion are those connecting different energy minima, known as double–well modes. Indeed, a one–to–one relation between the diffusion constant and the fraction f_{DW} of double–well modes has been observed in a range of model systems [7, 5, 8], We note that a different approach, where the modes contributing to diffusion are identified with the unstable and extended ones, and detected via a finite–size scaling analysis [9], has recently been shown to yield analogous results [6].

In order to investigate the relation between the features of the potential energy landscape and the diffusion constant of liquids, we focus on a simple model characterized by water-like density anomalies, i.e. regions of the phase diagram where the dynamics speeds up upon isothermal compression. We first consider two state points with the same diffusion constant D and same temperature, but different densities, and show that key dynamical features coincide at all length and time scales. Indeed, not only are the diffusion constants equal, but also the mean square displacements and the self-intermediate scattering (i.e. incoherent correlation) functions at different wavevectors coincide at all times. Differences are observed only in four–point quantities such as the non–linear dynamical susceptibility.

We then consider how the PEL changes with density, and how these changes are related to those in the dynamics. We show that the typical distance between two energy minima connected by a double–well mode, as well as the associated typical energy barrier, increase monotonically with density. Both quantities must thus be different for two state points at different density, even if they have the same diffusion constant. On the other hand, the fraction of unstable normal modes connecting different energy

minima $f_{\rm DW}$ varies non–monotonically with the density. This ensures it is correlated with the diffusion constant, but our results do not support the presence of a one–to–one relation between D and $f_{\rm DW}$ such as has previously been seen in other systems.

2. Model system

As a simple model system for investigating the relation between the dynamics and the features of the energy landscape we consider a polydisperse mixture of N harmonic disks of identical mass m, in two dimensions. Diameters are uniformly distributed in the range $[d_{\rm min}, d_{\rm max}]$, with the difference $d_{\rm max} - d_{\rm min}$ between the largest and smallest diameter being 82% of the mean diameter $(d_{\rm max} + d_{\rm min})/2$ so that the distribution is fairly broad; this is necessary to prevent crystallization. Two particles i and j interact via the repulsive harmonic potential

$$v(r) = \frac{1}{2}\epsilon \left(\frac{d-r}{d_{\rm max}}\right)^2 \tag{1}$$

The interaction is of finite range: particles interact only if their distance r is smaller than their average diameter $d = (d_i + d_j)/2$. Lengths, masses and energies are expressed below in units of $d_{\rm max}$, m and of ϵ, respectively, and the density is specified in terms of the volume (or more precisely, area) fraction $\phi = N\langle A\rangle/L^2$. Here L is the system size, $\langle A\rangle$ the average particle area, and N the number of particles.

We have performed molecular dynamics simulations [10] of this system with $N = 10^3$ particles, integrating the equations of motion using the Verlet algorithm, with a timestep of $\delta t = 10^{-4}$. Dynamical quantities are averaged over 10^3 independent runs. The system is first brought to thermal equilibrium via simulations in the NVT ensemble, while production runs are carried out in the NVE ensemble. Thermal equilibration is ascertained by checking for the absence of aging. The INMs are determined by equilibrating a larger sample, consisting of $N = 4 \times 10^3$ particles, and averaging over 50 independent realizations to obtain accurate statistics.

3. Density anomaly

In the majority of molecular and colloidal fluids the dynamics slows down upon isothermal compression. There are, however, fluids that display the opposite behavior in some region of their temperature–density phase diagram. Such density anomalies are found in a number of fluids; the most important of these is certainly water, with other examples including Si, Ge, Sn, and ionic melts with suitable radius ratios, such as SiO_2, BeF_2 and GeO_2 [11, 12]. While all of these systems have an anisotropic interaction potential that favors short-range tetrahedral order around the particle centers, density anomalies have been also observed in models with spherically symmetric interaction potentials [13]. These systems have been studied extensively to identify the physical origin of density anomalies and to connect them to specific features of the interaction potential. The harmonic potential considered in this work is an example

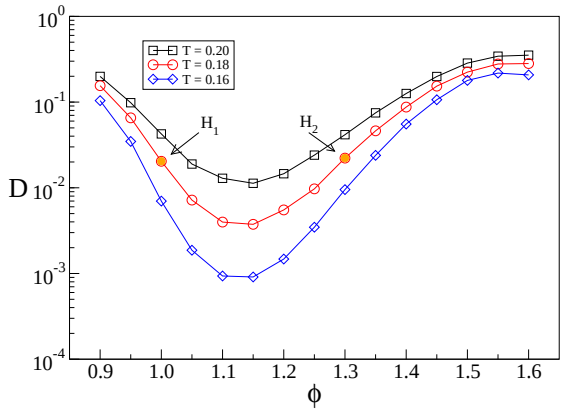

Figure 1. Non–monotonic density dependence of the diffusion constant. The arrows indicate the states $H_1 = (\phi = 1.0, T = 0.18)$ and $H_2 = (\phi = 1.3, T = 0.18)$, which have similar diffusion constants.

of a radially symmetric potential giving rise to a density anomaly, as illustrated by the non–monotonic dependence of the self–diffusion constant on volume fraction shown in Fig. 1. We have previously investigated the physical mechanisms responsible for this behavior, and concluded that it must be attributed to the emergence of contacts between a particle and those of its second coordination shell [14, 15]. In the following we first compare the dynamical features of two state points, $H_1 = (\phi = 1.0, T = 0.18)$ and $H_2 = (\phi = 1.3, T = 0.18)$, that have approximately the same diffusion constant, $D_{H_2}/D_{H_1} \simeq 1.13$ (Fig. 1), and then study the density dependence of some important features of the energy landscape.

4. Dynamics

As illustrated in Fig. 1, the presence of a density anomaly means that at a given temperature there are pairs of points that have different density but the same diffusion constant, such as state points H_1 and H_2. Due to the difference in density, one might expect the dynamics at these state points to be different in general, apart from sharing an overall timescale set by the diffusion constant. Surprisingly, we find that the opposite is true: state points with the same diffusion constant share many dynamical features. Consider first the mean square displacement shown in Fig. 2. It is equal between the two state points not only at long time, where this is expected because the two states have equal diffusion constant, but in fact at all times to within our numerical accuracy. This is consistent with the existence of a close link between the Debye–Waller factor, which is the value of the mean square displacement in the plateau region, and the diffusion constant. Such a link has been put forward on more general grounds [16], and we have previously verified that it applies across a large part of the phase diagram of the model system considered here [17]. The mean square displacement is given by the variance of the self part of the van Hove function, $G(r, t)$, defined here as

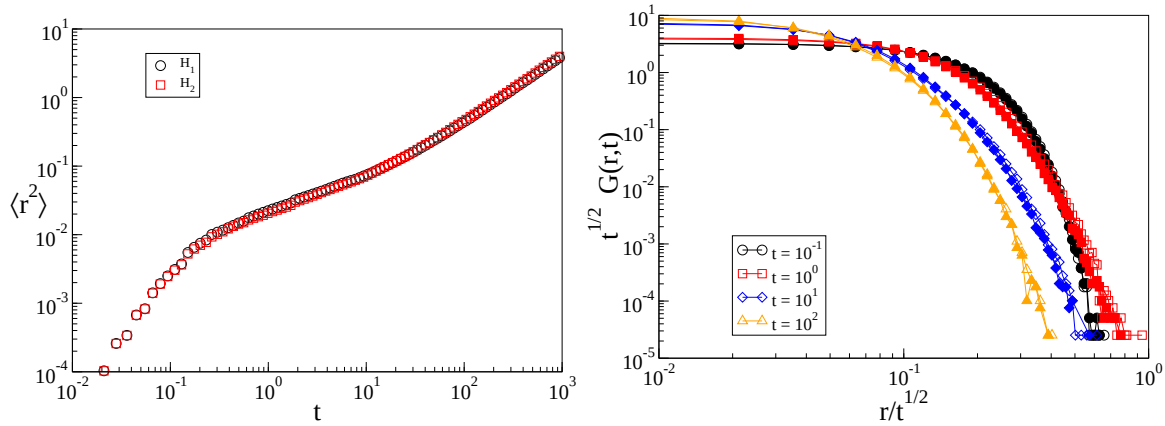

Figure 2. State points H_1 and H_2 have the same mean square displacement as a function of time (left panel), as well as the same van Hove correlation function for every time interval t (right panel), within numerical uncertainty.

the probability that a particle has moved a distance r along one coordinate (say x-)axis at time t. To investigate the relation between the dynamics at state points H_1 and H_2 more closely, we therefore next look at the van Hove function itself. Fig. 2 shows that, surprisingly, the van Hove functions — evaluated for the same time interval t – at H_1 and H_2 coincide not just in their variance, but in their entire functional dependence on r. The observed equality of the van Hove functions suggests that in fact the dynamics of the two systems might be equal at all relevant length scales. We have checked this by measuring the self–intermediate scattering (or incoherent correlation) function, $F(k,t) = \frac{1}{N}\left\langle \sum_{j=1}^{N} \exp\left[-i\boldsymbol{k}\cdot(\boldsymbol{r}_j(t)-\boldsymbol{r}_j(0))\right]\right\rangle$ for 11 different wavevectors $\boldsymbol{k}$ with lengths $k = |\boldsymbol{k}|$ evenly spaced between $k_{\max} = 4\pi/d_{\max}$ and $k_{\min} = 0.2\pi/d_{\max}$. As shown in Fig. 3, H_1 and H_2 have very similar self–intermediate scattering functions, at all times and length scales. Of course $F(k,t)$ is related to $G(r,t)$, essentially by Fourier transform, so this equality primarily provides a consistency check that equality of the dynamics is found both in real and Fourier space. We note that a similar collapse cannot be observed in the distinct part of the van Hove function, $G_d(r,t)$, as at $t = 0$ this coincides with the radial distribution function, which is distinct for states having different densities. Similarly, no collapse can be observed in the total–intermediate scattering function.

Digging deeper, differences in the dynamics at state points H_1 and H_2 finally turn up in the *fluctuations* of the self–intermediate scattering function. If we denote this fluctuating version of $F(k,t)$ by $\mathcal{F}(k,t) = \frac{1}{N}\sum_{j=1}^{N} \exp\left[-i\boldsymbol{k}\cdot(\boldsymbol{r}_j(t)-\boldsymbol{r}_j(0))\right]$ then its variance defines the so–called dynamical susceptibility $\chi(k,t) = N[\langle\mathcal{F}(k,t)\rangle^2 - \langle\mathcal{F}(k,t)^2\rangle]$. In this quantity we do find clear differences between H_1 and H_2, as shown in Fig. 3. In particular, while the susceptibilities attain their maximum roughly at the same time t^* for any given k, the actual maximal value $\chi(k,t^*)$ is smaller for state H_2, i.e. in the anomalous region.

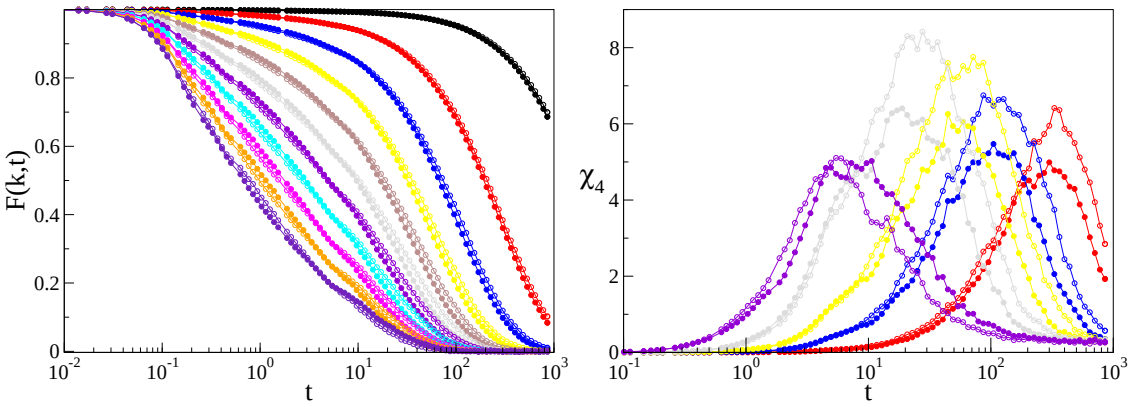

Figure 3. The left panel shows the self–intermediate scattering function, $F(k,t)$, for $k = k_{\min} + n(k_{\max} - k_{\min})/10$, and $n = 0, 1, .., 10$, from left to right. Here $k_{\min} = 0.2\pi/d_{\max}$ and $k_{\max} = 4\pi/d_{\max}$. Data for state point H_1 (full symbols) and H_2 (open symbols) coincide at all times and wavevectors, to a very good approximation. The right panel shows the corresponding dynamical suspeptibilities. For clarity, we only show data for $n = 0, 5, 7, 8, 9$, from left ro rigth.

5. Instantaneous normal–modes

Above we have found strong similarities between the dynamical properties of the equal-diffusion constant state points H_1 and H_2. If there is a significant correlation between the dynamics and the properties of the energy landscape, then this would suggest that the energy landscapes of states H_1 and H_2 should also have closely related features. More specifically this should apply to the statistics of those landscape properties that are directly related to the dynamics. Accordingly, by comparing different features of the energy landscape of the two states, we can infer to what extent they correlate with the dynamics.

To characterize the energy landscape statistics we employ the instantaneous normal mode approach, and thus focus on the properties of the eigenvalues λ_i and the eigenvectors $\boldsymbol{\delta u}_i$ of the Hessian matrix of the system. We consider first the distribution $P(\nu)$ of the eigenfrequencies $\nu_i = \sqrt{\lambda_i}$. These are shown in Fig. 4, where following the convention in the literature we plot imaginary eigenfrequences arising from negative eigenvalues λ_i as $-|\nu_i| = -\sqrt{|\lambda_i|}$. They can then be plotted on the same axis as the real eigenfrequencies, but remain distinct from them in such a visualization. Fig. 4 demonstrates clearly that the resulting two eigenvalue distributions differ between the state points H_1 and H_2. This is presumably driven by the difference in density between the two states.

The diffusive dynamics of the system, however, is not influenced by all modes. La Nave and coworkers [5] suggested that the unstable modes allowing for diffusion are the double–well modes, i.e. those connecting different energy minima, and observed a one–to–one relation between the diffusion constant D and the fraction of modes, f_{DW}, that have this double–well character. In order to determine if an unstable mode i is a

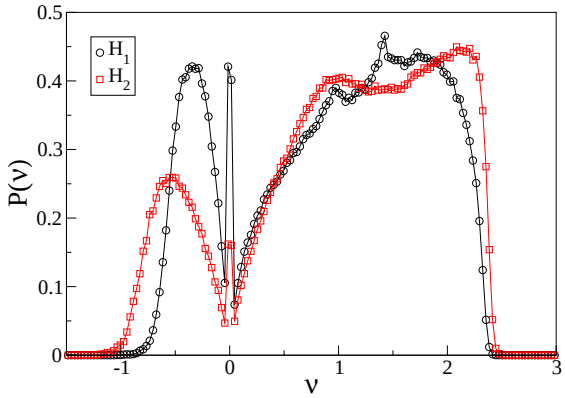

Figure 4. Probability distribution of the eigenfrequencies of state points H_1 and H_2, for a system of $N = 4,000$ particles. Imaginary eigenfrequencies ν are plotted as $-|\nu|$ to separate them from the real eigenfrequencies.

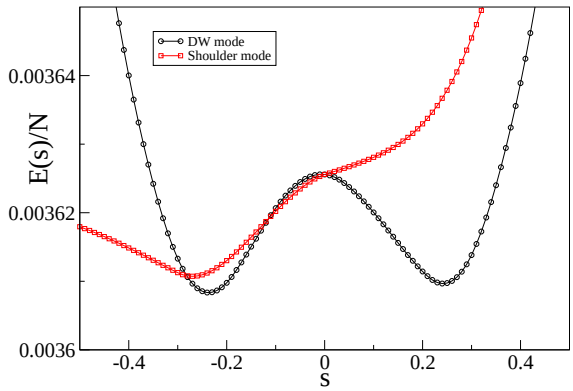

Figure 5. For each unstable eigenvalue i we have displaced the particle positions by an amounty $s\,\boldsymbol{\delta u}_i$ along the eigenvector $\boldsymbol{\delta u}_i$; the eigenvector is normalized so that s^2 gives the total squared displacement of all particles. The dependence of the energy of the system E on s allows one to discriminate between double–well modes and shoulder modes, as illustrated in the figure for two typical cases. The figure refers to state H_1 and $N = 4,000$.

double–well mode, one asks how the interaction energy of the system $E_i(s)$ changes as particles are displaced by $s\,\boldsymbol{\delta u}_i$ along the eigenvector. Note that, since we consider unit eigenvectors, s measures the distance the system is displaced in phase space: s^2 is the sum of all squared particle displacements. If $E_i(s)$ is a double–well function, i.e. has two local minima, then we classify the mode i as a double–well mode. As an illustration, we show in Fig. 5 numerical results for $E_i(s)$, for the two cases of a double–well and of a "shoulder" mode. We note that all modes with approximately zero eigenvalue, which are responsible for the observed peak in $P(\nu)$ around $\nu = 0$, turn out to be shoulder modes.

The features of the double–well modes change with density. As displayed in Fig. 6, the average distance $\langle dr \rangle$ separating two energy minima in phase space and

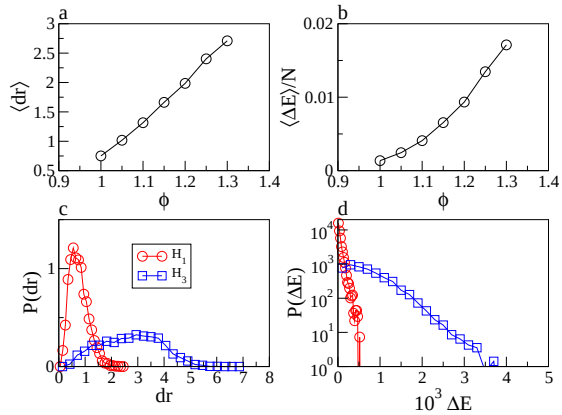

Figure 6. Bottom row: Probability distribution of the distance dr between two energy minima connected by a double–well mode (bottom left), and of the energy barrier ΔE separating the two minima (bottom right), for the two states H_1 and H_2. Top row: averages of these quantities as a function of volume fraction, across the range between H_1 ($\phi = 1$) and H_2 ($\phi = 1.3$).

the corresponding average energy barrier $\langle \Delta E \rangle$, increase monotonically with density. In particular, these quantities are therefore not identical for the two states H_1 and H_2, suggesting that they are at most weakly correlated with the dynamics. The figure (bottom row) also show that dr is approximately Gaussian distributed, while ΔE has a roughly exponential distribution. We already know the averages of the two distributions are different for H_1 and H_2, and accordingly also the distributions themselves are quite distinct.

So far we have found for the instantaneous normal mode eigenfrequency distribution, and geometrical properties of double–well modes such as distance and barrier between the two minima, that states H_1 and H_2 show clear differences in their energy landscape statistics. We now turn, finally, to the fraction f_{DW} of double–well modes. As shown in Fig. 7a, this varies non–monotonically with the volume fraction, much like the diffusion constant. As expected, a parametric plot of D versus f_{DW} in Fig. 7b therefore exhibits a strong correlation between these two quantities. The fraction of double–well modes is therefore clearly one feature of the energy landscape that is closely linked to the dynamics, and indeed (Fig 7a) its values in states H_1 and H_2 are within $\approx 23\%$ of each other. However, Fig 7b also demonstrates that for our system there is no one–to–one correspondence between D and f_{DW}, in contrast to what has been observed in other systems [5].

6. Conclusions

We have investigated a polydisperse mixture of disks interacting via a repulsive finite-range harmonic potential, in the volume fraction and temperature range where the system displays a density anomaly. We have focussed primarily on the possible existence

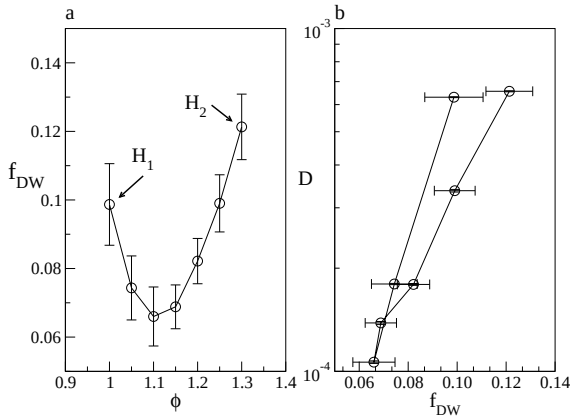

Figure 7. (a) The fraction f_{DW} of unstable modes connecting different energy minima, i.e. double-well modes, varies non–monotonically with the volume fraction. (b) It is therefore strongly correlated with the diffusion constant, but does not determine it uniquely.

of correlations between the dynamics and features of the potential energy landscape. We have observed striking similarities between the dynamical features of state points characterized by the same diffusion constant: as far as can be ascertained from incoherent (i.e. single particle) two-point correlations, their dynamics appear to coincide at all length and time scales. We note that these dynamical similarities are not confined to the two specific state points $H_1 = (\phi = 1, T = 0.18)$ and $H_2 = (\phi = 1.3, T = 0.18)$ that we have studied; we have obtained analogous results when comparing e.g. the dynamics at the state points $(\phi = 1.03, T = 0.16)$ and $(\phi = 1.25, T = 0.16)$. What is the physical origin of these dynamical similarities is not obvious to us, and will be an interesting question to follow up in future work. In this respect, we mention also that not all liquids with density anomalies have this feature; indeed, for a repulsive Gaussian interaction we generally find quite distinct dynamics for states of equal diffusion constant [18].

Despite the dynamical similarities we have found in our specific model system, the states that are paired up by having equal diffusion constant have PELs with quite different statistics. These include the average distance between minima connected by unstable normal modes, and the average barrier. One quantity where we do find a strong correlation with the dynamics is in the fraction f_{DW} of double–well modes among all instantaneous normal modes; such double–well modes are defined as unstable modes connecting different energy minima. However, while there is a clear correlation between f_{DW} and D, the two quantities are not uniquely determined by each other. This suggests that in our system there must be other features of the landscape, beyond f_{DW}, that act to determine the diffusion constant D.

7. Bibliography

[1] T. Keyes, J. Phys. Chem. A **101**, 2921 (1997).
[2] R. LaViolette and F. H. Stillinger, J. Chem. Phys. **83**, 4079 (1985); R. Cotterill and U. Masden, Phys. Rev. B **33**, 262 (1986).
[3] F. Sciortino and P. Tartaglia, Phys. Rev. Lett. 78, 2385 (1997).
[4] J. D. Gezelter, E. Rabani, and B. J. Berne, J. Chem. Phys. **12** 107 (1997).
[5] E. La Nave, A. Scala, F.W. Starr, F. Sciortino and H.E. Stanley, Phys. Rev. Lett. **84**, 4605 (2000).
[6] V.I. Clapa, T. Kottos and F.W. Star, J. Chem. Phys. **136**, 144504 (2012).
[7] W. -X. Li and T. Keyes, J. Chem. Phys. **111**, 5503 (1999).
[8] E. Salcedo, A. Barros de Oliveira, N. M. Barraz Jr, C. Chakravarty and M. C. Barbosa, J. Chem. Phys. **135**, 044517 (2011).
[9] S. D. Bembenek and B. B. Laird, Phys. Rev. Lett. **74**, 936 (1995); J. Chem. Phys. **104**, 5199 (1995).
[10] S. Plimpton, J. Comp. Phys **117**, 1 (1995).
[11] J. S. O. Evans, J. Chem. Soc., Dalton Trans. 3317 (1999).
[12] W. Miller, C. W. Smith, D. S. Mackenzie, and K. E. Evans, J Mater Sci **44**, 5441 (2009).
[13] S. V. Buldyrev, G. Malescio, C. A. Angell, N. Giovambattista, S. Prestipino, F. Saija, H. E. Stanley, and L. Xu, Journal of Physics: Condensed Matter **21**, 504106 (2009).
[14] M. Pica Ciamarra and P. Sollich, Soft Matter **9**, 9557 (2013).
[15] M. Pica Ciamarra and P. Sollich, J. Chem. Phys. **138**, 12A529 (2013).
[16] J.J. Dyre, Rev. Mod. Phys. **78**, 953 (2006).
[17] M. Pica Ciamarra and P. Sollich, Journal of Non-Crystalline Solids **407**, 23 (2015).
[18] P. G. Debenedetti, V. S. Raghavan, and S. S. Borick, J. Phys. Chem. B **95**, 4540 (1991).